Inkjet Bioprinting of 3D Silk Fibroin Cellular Constructs using Sacrificial Alginate

Ashley M. Compaan[1], Kyle Christensen[2], Yong Huang[1,2,*]

[1]Department of Materials Science and Engineering, University of Florida, Gainesville, FL 32611, USA

[2]Department of Mechanical and Aerospace Engineering, University of Florida, Gainesville, FL 32611, USA

*Corresponding author, Department of Mechanical and Aerospace Engineering, University of Florida, Gainesville, FL 32611, USA, Phone: 001-352-392-5520, Fax: 001- 352-392-7303, Email: yongh@ufl.edu

Abstract

Silk fibroin is a natural protein which has shown great promise for tissue engineering, but is not printable due to slow gelation or harsh gelation conditions which are not cell-friendly. In this study, a two-step gelation process is proposed for the printing of silk fibroin, which utilizes alginate as a sacrificial hydrogel during an inkjetting-based process. A cell-laden blend of alginate with silk fibroin is utilized to achieve rapid gelation by calcium alginate formation during printing; it is followed by horseradish peroxidase (HRP) catalyzed covalent crosslinking of the fibroin protein at tyrosine residues after printing. This two-step gelation process successfully enables 3D bioprinting of well-defined cell-laden silk fibroin constructs suitable for long term culture. The constructs remain intact after calcium chelation to liquefy the alginate

component, demonstrating the formation of silk fibroin hydrogel. NIH 3T3 fibroblasts proliferate and spread through the hydrogel after printing. Increasing metabolic activity is observed for 5 weeks after printing, and histology shows dense cell populations in cultured constructs. The proposed two-step gelation technique is expected to enable 3D silk fibroin printing for various applications.

Keywords: Silk fibroin, 3D bioprinting, two-step gelation, sacrificial material, alginate, horseradish peroxidase

1. Introduction

Enabled by advances in engineering and cellular biology, three dimensional (3D) bioprinting has recently emerged as an important tissue engineering tool, aiming to construct functional biological structures for various medical applications[1-3]. Two primary applications of such constructs are: clinical applications in regenerative medicine[4] and research tools for pre-clinical, diagnostic, and developmental studies[5]. As a freeform fabrication approach, 3D bioprinting is capable of generating porous living constructs with pre-determined heterogeneity on demand and therefore has great potential to produce a suitable architecture for functional tissues with adequate mass transport to encapsulated cells.

For bioprinting to be a viable technology, material development for bioprinting is as important as the development of fabrication processes[6-12]. In terms of printability, such materials should be flowable or deformable in order to be deposited in addition to being biocompatible and biodegradable; after printing, they should retain the shape as printed, and the chemical and/or

physical mechanisms resulting in shape conservation must be compatible with living cells[13-16]. In terms of *in vitro* or *in vivo* performance, some biomaterials which closely mimic native tissues, such as collagen and fibrin, are rapidly contracted and distorted *in vitro*, so the designed architecture is easily lost[17]; on the other hand, synthetic materials may provide better control over construct shape and properties but lack chemical and microstructural features to direct cell functionality.

Recently, silk fibroin, a natural protein from a non-mammalian source, has been extensively studied for tissue engineering applications[18-21]. In particular, silk fibroin is valuable for long term *in vitro* studies, where a stable matrix having well-defined mechanical and physical properties is necessary[21]. Many constituents of native extracellular matrix are remodeled too rapidly to be of use for such applications; in contrast, silk is robust enough to maintain its original morphology over many weeks of culture while supporting normal cell functions including spreading, migration, and proliferation. Silk fibroin degrades slowly[22-24] and effectively supports cell functionality[25]. While chemical modifications of silk fibroin are possible and have been explored, the native fibroin protein does not require any additional functionality to generate various stable constructs for tissue engineering[20]. Silk fibroin contains approximately 5% tyrosine residues[18] bearing phenol functional groups; in the presence of trace amounts of hydrogen peroxide, the enzyme horseradish peroxidase (HRP) forms a covalent bond between two such residues, resulting in a covalently crosslinked hydrogel[26]. Physical silk fibroin hydrogels can also be generated by promoting crystallization of silk fibroin protein via vortex mixing[27], sonication[28], or solvent exposure[29-31].

As a promising biomaterial, silk fibroin has been utilized to fabricate 3D periodic grid constructs[28-31]. To fabricate mechanically stable, gelled constructs, these extrusion-based 3D fabrication methods utilize either cytotoxic conditions which promote the crystallization of protein for effective gelation[29-32] or a silk fibroin solution in which crosslinking is initiated before fabrication[28]. In the former case, deleterious conditions used during fabrication include methanol exposure[29-31] and freeze drying[32]. Both treatments promote secondary structures which are insoluble in water, but unfortunately neither treatment is compatible with living cells. In the latter case[28], the ink rheological properties change continuously during printing due to ongoing gelation (enzymatic crosslinking and physical interactions), making the printing process difficult to control. Unfortunately, freeform bioprinting of truly 3D constructs has not been possible because most silk gelation mechanisms are too slow (on the order of minutes to hours) to form a defined hydrogel construct unless using cytotoxic conditions[29-32] or pre-gelled silk fibroin ink[28] as described above. It is noted that inkjet printing of 2D fibroin patterns has been reported[33, 34] in which stable motifs were formed after the printed solution dried to form a film; however, this process is also incompatible with living cells since it involves desiccation to stabilize the printed films. While the acellular scaffolds achievable with existing methods have value, it is difficult to homogeneously and efficiently seed cells post-fabrication[24], and spatially-defined seeding of multiple cell types is impossible. It is of great importance to keep the excellent *in vitro* and *in vivo* performance of silk fibroin hydrogel while improving the printability of silk fibroin for cell encapsulation.

The objective of this study is to demonstrate the feasibility of using silk fibroin to freeform fabricate 3D cellular constructs via a two-step gelation process, which utilizes alginate as a

sacrificial hydrogel during an inkjetting-based process. To that end, a silk fibroin-alginate bioink is prepared and investigated for 3D bioprinting, which is made possible using a two-step gelation approach: first near-instantaneous ionic gelation of sodium alginate on contact with calcium chloride, and second covalent gelation via the enzymatic crosslinking of the silk fibroin protein entrapped in the calcium alginate construct. Sacrificial alginate provides structural definition during printing and may be removed later by mild chelating agents such as sodium citrate or ethylenediaminetetraacetate (EDTA). Its excellent performance in freeform fabrication applications is well documented[8-11, 13-14, 25, 35-37]; in addition, it can be gelled and liquefied without damaging encapsulated cells or interfering with the enzymatic crosslinking of silk fibroin. In contrast to other additives[28-32] which have been reported to facilitate silk fibroin construct formation, alginate gelation is easy to control and does not require desiccation or solvent exposure; this blend is therefore suitable for the direct fabrication of cell-laden constructs. As a non-toxic and FDA approved material[38], residual alginate has little impact on the functional or clinical potential of this approach. While alginate is selected as the sacrificial material in this study due to its rapid gelation, other sacrificial materials may also be explored. The proposed two-step gelation technique is expected to enable 3D silk fibroin printing for various applications.

2. Materials and Methods

2.1 Bioink preparation

Aqueous silk fibroin (5%, Advanced Biomatrix, San Diego, CA) was stored at -80°C, and an aliquot was thawed immediately before use. HRP (Type I, essentially salt free, Sigma-Aldrich, St. Louis, MO) stock solution was prepared at a concentration of 5000 U/mL in deionized water

and stored frozen at -20°C until use. Alginate stock solution was prepared by dissolving sodium alginate (450-550 kDa, Acros Organics, NJ) at a concentration of 5% in 10× phosphate buffered saline (PBS) (10× Dulbecco's PBS without Ca and Mg cations, MP Biomedicals, Solon, OH). The bioink was prepared by mixing these solutions to obtain final concentrations of 4.5% silk fibroin, 200 U/mL HRP, and 0.5% sodium alginate. As needed, 1M HCl was used to adjust the pH to 7. NIH 3T3 mouse fibroblasts (ATCC, Rockville, MD) were maintained as described previously[8]. For cellular ink preparation, harvested cells were washed with 1× PBS to remove media, centrifuged, and re-suspended in the hydrogel precursor mixture at 5×10^6 cells/mL. A non-toxic surfactant, Pluronic L101 (BASF, Florham Park, NJ)[39], at a concentration of 0.005% w/v, was also included in ink formulations to reduce foaming and cell settling. As noted elsewhere[40], silk fibroin and alginate are not fully miscible, so the ink mixture could not be prepared in advance since it may gradually separate into two distinct phases. Fortunately, when used promptly, ink remains homogeneous. During printing, the bioink mixture should be pipetted gently every 15-20 min to mitigate cell settling while re-mixing the hydrogel components.

2.2 Three-Dimensional Printing

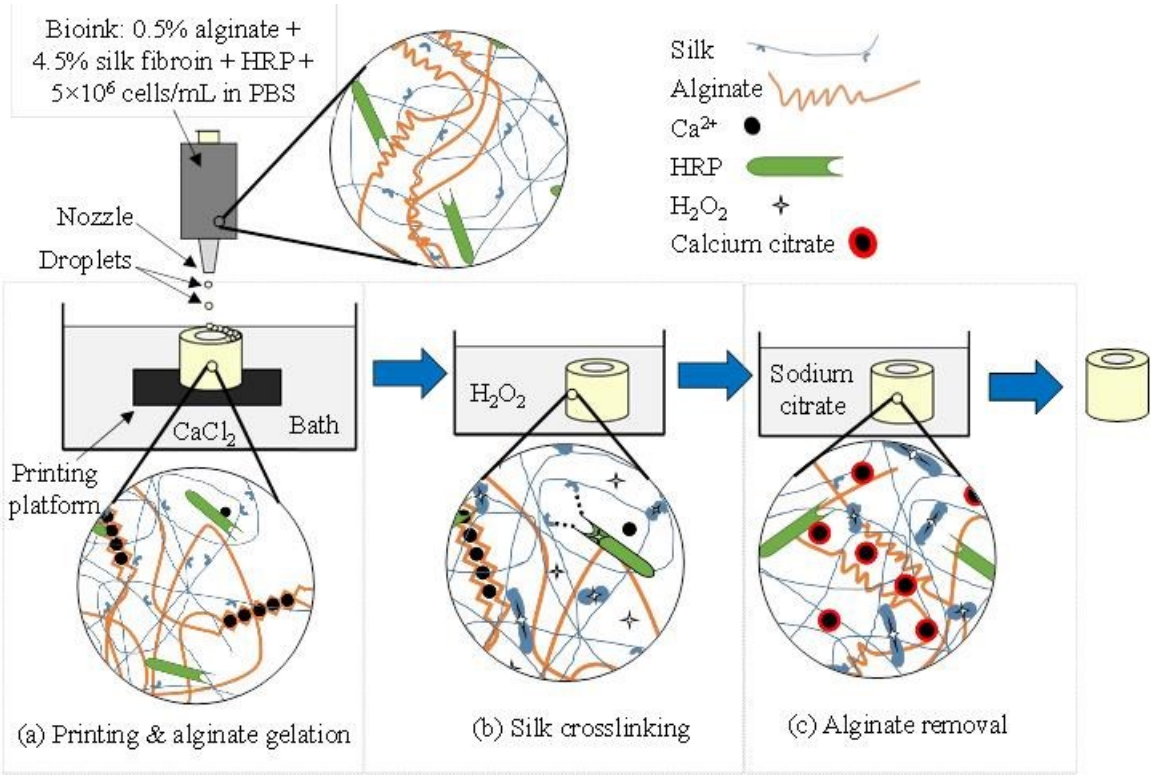

Figure 1. Schematic of 3D printing with inset schematic of mixed components of bioink (cells not shown). (a) Printing process with inset schematic of printed bioink showing typical egg-box ionic calcium alginate gel with entrapped silk fibroin and HRP. (b) HRP-catalyzed silk fibroin crosslinking in H_2O_2 bath. (c) Alginate gel disrupted by sodium citrate treatment, leaving a crosslinked silk fibroin gel construct.

Silk constructs were fabricated with a previously described piezoelectric inkjet 3D printing system[8, 9, 35, 36] based on a two-step gelation approach. The key innovation is the use of fast-gelling alginate as a sacrificial material to maintain the structural integrity of constructs being printed since enzymatic silk fibroin gel cannot form rapidly enough to build well-defined 3D constructs. As illustrated in Figure 1, the silk-alginate mixture is firstly used to form the desired geometry as a result of immediate alginate gelation (Figure 1(a)). Sodium alginate, which gels

almost instantaneously when exposed to divalent cations such as calcium, is added to the bioink to enable gelation of well-defined constructs as printed. Then, the construct is transferred to a second crosslinking bath for 10 minutes for horseradish peroxidase (HRP)-catalyzed crosslinking of tyrosine residues along the silk fibroin chain to generate a covalently crosslinked, cell-laden, stable silk fibroin construct (Figure 1(b)). As needed, alginate can be removed using mild chelating agents such as sodium citrate or EDTA (Figure 1(c)) to achieve a silk fibroin construct, which would have otherwise been difficult or impossible to fabricate due to the slow gelation rate of silk fibroin.

During fabrication, each layer was formed as a 120 μm nozzle (MicroFab, Plano, TX) traveling at 5 mm/sec deposited droplets of the bioink at 60-120 Hz along designed print paths. Layers were deposited consecutively onto a platform[9] which was lowered by a *Z* translational stage (Aerotech, Pittsburgh, PA) into an initial crosslinking solution of 2% w/v $CaCl_2$•$2H_2O$ (Sigma-Aldrich, St. Louis, MO) as shown in Figure 1(a). As each layer was completed, the construct was lowered into the bath by the thickness of the layer, such that the top of the construct remained at the surface of the bath solution, which facilitated the formation of a calcium alginate hydrogel with entrapped silk fibroin. Printing time varied with construct size and shape, and was between 5 and 10 minutes for tubular constructs (5 mm diameter, 2.5 to 5.0 mm height) fabricated herein.

2.3 Post-printing treatment

Printed constructs were immediately transferred to aqueous 4.4 mM (0.015%) H_2O_2 (from 3% solution, Swan, Smyrna, TN) in 2% $CaCl_2$•$2H_2O$ for HRP catalyzed silk crosslinking. As observed, a long delay (such as 1 hour) between printing and H_2O_2 treatment resulted in weak

constructs after citrate treatment, likely due to the diffusive loss of HRP to the $CaCl_2$ bath and resulting inadequate silk fibroin crosslinking. It should be noted that a higher HRP concentration in bioinks may mitigate this problem if there is a long delay between printing and H_2O_2 treatment. Alternatively, HRP could be mixed with the bath rather than the bioink to make crosslinking conditions more consistent instead of dependent on the processing time before H_2O_2 exposure. However, placing HRP in the bath would likely result in only surface crosslinking of the silk fibroin construct since the large enzyme (~44 kDa) cannot reach the interior of printed constructs effectively and efficiently. The low concentration of H_2O_2 (0.015%) adopted in this study is only mildly toxic to unprotected cells[41]; furthermore, as it diffused into printed constructs, H_2O_2 was consumed by the crosslinking reaction so encapsulated cells were exposed to an even lower concentration of H_2O_2.

After enzymatic crosslinking, printed constructs were placed in sterile aqueous 1.62% sodium citrate (molecular biology grade, VWR, West Chester, PA) for 30 minutes to remove alginate. For comparison, additional printed constructs were not treated with sodium citrate. Citrate-treated and non-citrate-treated constructs were cultured separately to evaluate whether the removal of alginate affects the structural stability or cell proliferation.

For incubation, each printed construct was transferred to a well of a 24 well plate with 1 mL of normal growth media, which consisted of Dulbecco's modification of Eagle's Medium (DMEM, Corning Cellgro, Manassas, VA) supplemented with 10% fetal bovine serum (FBS, Hyclone, Logan, UT) and 1% antibiotic antimycotic solution (Antibiotic Antimycotic Solution (100×), Stabilized, Sigma-Aldrich, St. Louis, MO).

2.4 Material characterization

Scanning electron microscopy (SEM) was utilized for the observation of resulting construct microstructure. Acellular tubes were printed as described for cellular tubes but omitting cells during the ink preparation. Some tubes were treated with 1.62% citrate for 30 minutes to remove alginate after crosslinking with both $CaCl_2$ and H_2O_2. All were rinsed with DI water to remove excess salt and frozen at -80°C for 12 hours before freeze drying. The freeze dried constructs were mounted on stubs, double coated with carbon, and imaged using a desktop SEM (Phenom Pro-X, Phenom-World B.V., Endhoven, Netherlands) at a voltage of 15 kV.

For mechanical property characterization, tensile testing was conducted for three types of samples: alginate only, alginate/silk fibroin mixture without citrate treatment, and alginate/silk fibroin mixture with citrate treatment. Specifically, six dog-bone shaped samples (1.5 mm thick, 2.5 mm gauge width, and 6 mm gauge length) were cast in poly(dimethylsiloxane) molds from acellular ink solutions (4.5% silk fibroin, 0.5% alginate, 0.005% L101, 200 U/mL HRP, in PBS) and crosslinked using 2% $CaCl_2 \cdot 2H_2O$ with 4.4mM H_2O_2. Three of six cast gels were placed in 1.62% sodium citrate solution for 30 minutes to remove alginate immediately before testing. Three alginate-only samples were also fabricated from 0.5% alginate in PBS for comparison. After excess water removal by blotting, each sample was clamped in an eXpert 4000 MicroTester testing system (Admet, Norwood, MA) and stretched at 0.05 mm/sec while recording load on a 50 g load cell for 10 mm or until failure. The Young's modulus was determined based on the slope of the linear region of the force-elongation curve and the sample geometry.

2.5 AlamarBlue assay

The cellular activity in incubated constructs was evaluated using the alamarBlue assay at various time points up to 42 days after printing. In the reducing environment of living cells, the blue non-fluorescent resazurin dye is converted to fluorescent pink resorufin; the fluorescent intensity after a defined incubation period is proportional to the cell population. Because it is nontoxic, the same sample can be assayed repeatedly to obtain data over time without sample-to-sample variation affecting results. Each well, containing a single construct in 1 mL culture media, was treated with 100 μL of alamarBlue (Thermo Scientific, Rockford, IL) and incubated for 4 hours at 37°C with 5% CO_2. Then, the media from each well was carefully transferred to a separate plate to avoid the influence of hydrogel in the detection area, and read immediately using a microplate reader (Synergy HT, Biotek, Winooski, VT; fluorescent excitation 530 nm/emission 590 nm) at 37°C. Fluorescence data was exported to Microsoft Excel for processing.

2.6 Fluorescent imaging

Fluorescein diacetate (FDA) (Sigma-Aldrich, St. Louis, MO) was used to stain live cells for fluorescent imaging (EVOS FL, Grand Island, NY), and Hoescht 33342 (Life Technologies, Eugene, OR) was used to counterstain nuclei blue. Constructs were rinsed with 1× PBS, then incubated in PBS containing 50 ng/mL FDA and 1.2 ng/mL Hoescht 33342 for 10 minutes at room temperature before imaging. Both fluorescent and transmitted light images were collected at various time points after printing using microscopy (EVOS FL, Grand Island, NY).

For comparison of cell morphologies, cell-laden alginate gel (0.5% w/v in PBS) and silk-alginate gel (0.5% alginate and 4.5% silk fibroin in PBS) were formed by pipetting 20 μL aliquots of the

appropriate precursor into a 2% $CaCl_2$•$2H_2O$ bath. After 10 minutes, all gels were transferred to a second $CaCl_2$ bath containing 4.4 mM H_2O_2 for another 10 minutes. Then, they were transferred to fresh aqueous 2% $CaCl_2$•$2H_2O$ without H_2O_2 for an additional 10 minutes. Finally, half of the silk and alginate gels were transferred to sterile 1.62% sodium citrate for 30 minutes to remove alginate. All constructs were cultured for one day in DMEM supplemented with FBS and antibiotics as described for printed constructs and stained with FDA for microscopic examination.

2.7 Histology

Printed constructs immediately after printing and cultured for 50 days were fixed, equilibrated in PBS (twice, 15 minutes each), and stored in fresh PBS before histological processing. The constructs were dehydrated, embedded in paraffin, sectioned (4 μm), and stained with hematoxylin and eosin (H&E). Sections were observed and imaged using a digital color microscope in brightfield mode (EVOS XL, Grand Island, NY).

3. Experimental Results and Discussion

3.1 Printed constructs

Various tubular constructs, the simplified basic unit of vascular structures[8, 35-36], are successfully printed using the proposed two-step gelation process. For easy handling and examination, the tubular constructs herein have a diameter of 5 mm and a height of 2.5 or 5.0 mm. The resulting tube thickness is on the order of 400 μm. Figure 2(a) and 2(b) shows the homogeneous distribution of living cells, stained with Hoescht 33342 and FDA, respectively, for all and living cells within a construct immediately after printing. As illustrated in Figure 2(c)-(f), there is no

noticeable change in construct appearance during the long culture period. The constructs hold their shape well and are easy to handle; even after 6 weeks in culture with embedded cells, the printed tubes are capable of supporting their own weight in air, indicating that citrate-treated silk fibroin hydrogel can maintain the structural integrity of printed constructs. For comparison, some non-citrate treated constructs are also incubated and examined, and there is no pronounced shape difference between the citrate-treated and non-citrate treated tubular constructs. It is concluded that the structural integrity is not affected by the removal of alginate. It should be noted that such silk fibroin hydrogels retain structural integrity from weeks to months[22-24, 26], and future study may include degradation experiments to confirm this behavior.

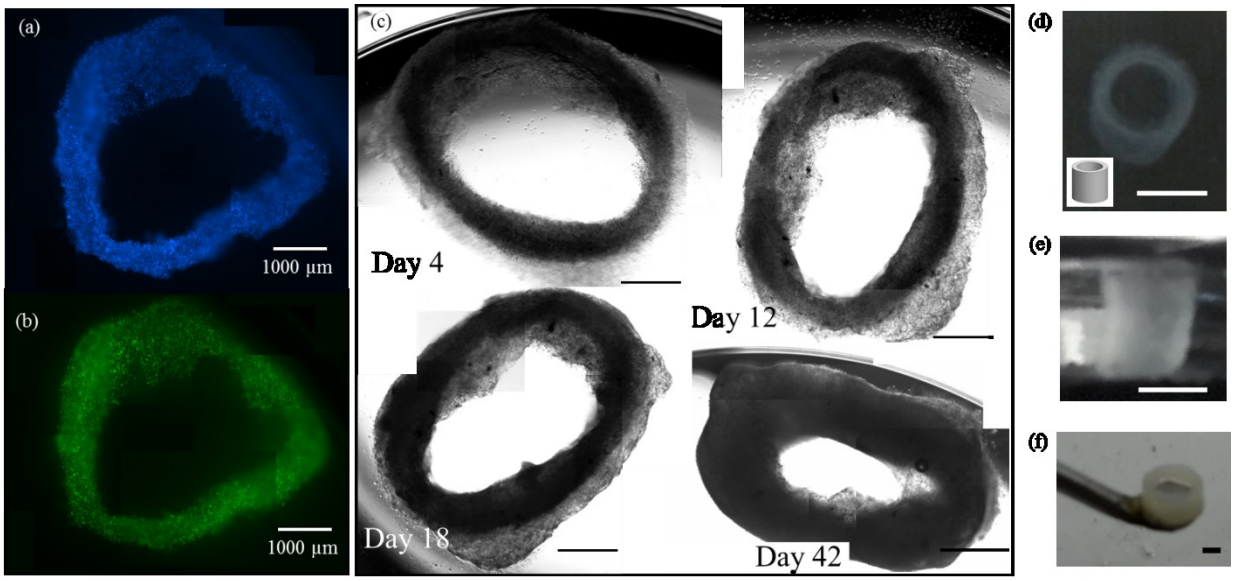

Figure 2. (a) Hoescht 33342 and (b) FDA stained printed citrate-treated constructs on Day 0. (c) Micrographs of an incubated construct on Days 4, 12, 18, and 42, reconstructed from multiple images (scale bar: 1 mm). (d) Top view of a 5-mm high tube immediately after printing (Inset: design schematic and scale bar: 3 mm) (e) Side view of the tube from (d). (f) Macroscopic view of a printed 2.5-mm high tube after eight-day incubation (scale bar: 1 mm).

3.2 Material characterization results

Both non-citrate-treated and citrate-treated constructs are porous as shown in Figure 3. Non-citrate-treated constructs have a more fibrous and open microstructure, while citrate-treated constructs show generally smooth-walled pores with fewer inter-connections. The higher inter-connectivity in non-citrate-treated constructs is attributed to microscale phase separation between alginate and silk fibroin as well as differences in ice crystal formation during freezing as a result of heterogeneities which provide nucleation points[42]. The latter is likely more significant since the microscale heterogeneities in polymer composition are present in all constructs and fixed by the gelation process prior to citrate treatment. That is, any features arising from the ink preparation and crosslinking process should be similar in both cases since these features are preserved before citrate treatment. A similar trend of increasing fibrous character with increasing alginate content has been observed in other freeze-dried silk fibroin-alginate blends[43]. In addition, a very large cavity is visible in Figure 3(b), which is likely a result of a gas bubble in the original gel as a result of HRP catalyzed H_2O_2 decomposition.

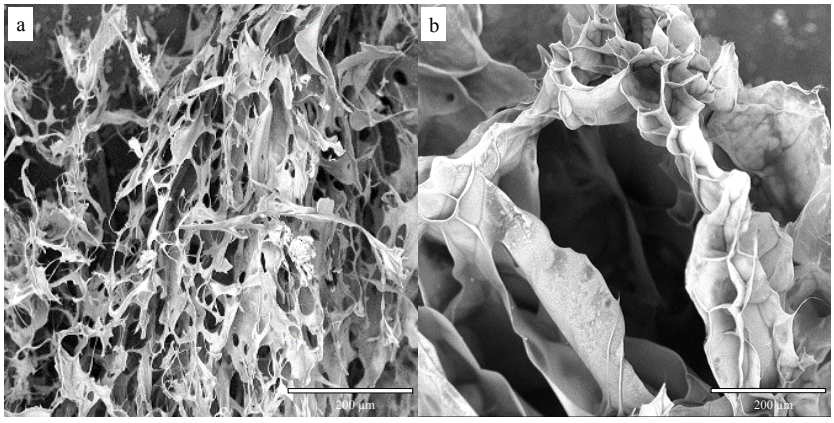

Figure 3. SEM images of acellular constructs: (a) non-citrate treated and (b) citrate treated (showing a large cavity likely formed by an air bubble).

The Young's moduli of alginate samples, alginate/silk fibroin samples without citrate treatment, and alginate/silk fibroin samples with citrate treatment are 9.0 ± 0.9 kPa, 7.5 ± 1.8 kPa, and 6.6 ± 0.4 kPa, respectively, showing that the silk-containing samples are less stiff than alginate and the removal of alginate makes the samples elastic. As observed, the silk-containing samples have a good elastic recovery while alginate samples are permanently deformed. These measurements are consistent with data reported for HRP-crosslinked silk fibroin in compression[26] and of the same order of magnitude as reported for concentrated alginate gels[11].

3.3 Post-printing metabolic activity

The alamarBlue results show that the printed constructs, both citrate treated and non-citrate treated, provide a hospitable environment for 3T3 cell growth and proliferation. As seen from the alamarBlue assay data in Figure 4, the post-printing metabolic activity of citrate-treated constructs increases rapidly up to Day 33 then decreases slowly. This observation illustrates that encapsulated cells in the printed silk fibroin hydrogel constructs are not only alive but also proliferating. The observed increasing metabolic activity during the first 33 days is indicative of adequate porosity left by alginate removal, allowing cells to spread and proliferate through the volume of the constructs rather than restricting them to their deposited locations. As cells further proliferate, they may form dense cellular surface layers, blocking nutrient and oxygen diffusion to cells further from the surface. This leads to the slight decline in metabolic activity near the end of the 42-day culture period. A similar pattern of rapid growth followed by slow decline is commonly reported for the long-term culture of different cell types including fibroblasts[42, 44] using silk fibroin matrices[26, 45].

Interestingly, little difference in metabolic activity is observed between printed constructs treated and not treated with citrate to remove alginate. Generally, the metabolic activity of citrate-treated constructs is higher than that of non-citrate-treated constructs. In particular, this discrepancy is large during the first two weeks of incubation since citrate-treated constructs have a porous structure providing more channels for nutrient and oxygen exchange, which is necessary for good cell proliferation. After two weeks, the metabolic activity of the two types of constructs is similar. This is attributed to the relatively rapid loss of alginate to culture media as calcium is chelated by phosphate and other buffers to provide additional mass transport channels; it is reported that calcium alginate constructs may lose structural stability after a week of incubation[37].

The slightly lower maximum metabolic activity in non-citrate-treated constructs may be due to earlier formation of a dense cell layer on the tube surface, where alginate would be lost first, and less proliferation in the interior of construct wall due to the combination of residual alginate and limited nutrition. In contrast, citrate-treated constructs support similar proliferation throughout the wall thickness, so the cell population in construct walls increases along with the surface cell population, resulting in a higher maximum. Once the cell population starts to decline, the two construct types have a similar level of metabolic activity since both have similar surface areas for active cells.

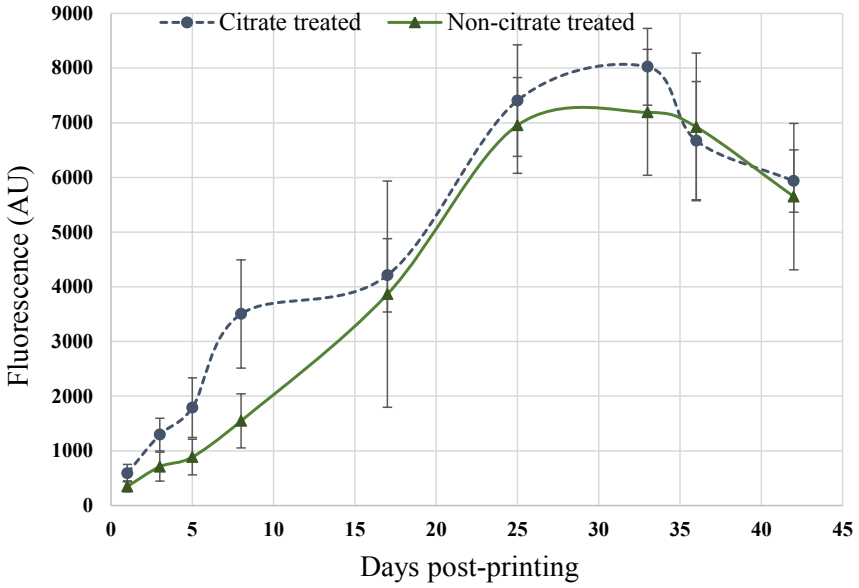

Figure 4. alamarBlue data for cultured printed constructs with ±1σ error bars for three replicates.

3.4 Cell morphology

For illustration, the cell morphology is observed using fluorescent microscopy. Figure 5 shows typical cell morphologies one day after encapsulation in pipetted gels of 0.5% alginate, non-citrate-treated 0.5% alginate and 4.5% silk fibroin, and citrate-treated 0.5% alginate and 4.5% silk fibroin. While the green fluorescence shows that live cells are abundant in all three cases, alginate holds cells trapped in their original round morphology, and cells remain isolated. As observed, there is no noticeable difference in terms of the cell morphology between the non-citrate-treated and citrate-treated alginate and silk fibroin hydrogels. The presence of silk, whether mixed with alginate or after alginate removal by citrate treatment, enables cells to extend and make contact with one another, generating a cellular network throughout the hydrogel volume. The lack of spatial confinement also permits rapid proliferation, as indicated by the almarBlue data in Figure 4. Similar results are reported when culturing mammalian cells in/on

silk fibroin materials[25, 26, 43, 46, 47]. Such cell proliferation and cellular interactions are essential for tissue formation; cells should communicate with each other directly in order to form a functional tissue-like construct[48, 49]. Matrices which support cell adhesion and spreading also enhance differentiation[50] and functionality[51, 52]. Since the silk-alginate blends employed in this work support excellent cell adhesion and network formation, they can also be expected to support the functionality and/or differentiation of encapsulated cells, which is a topic for future work.

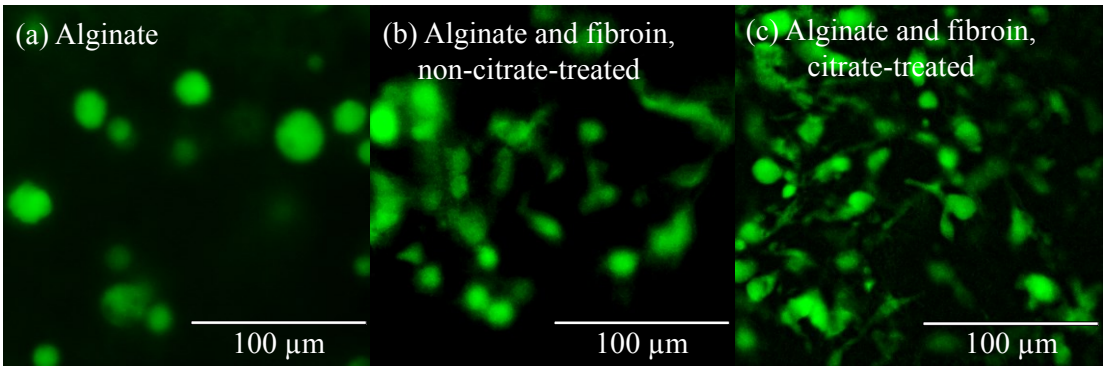

Figure 5. FDA stained 3T3 cells in (a) alginate, (b) non-citrate-treated alginate and silk fibroin, and (c) citrate-treated alginate and silk fibroin constructs after one-day incubation.

3.5 Histology study

As seen from Figure 6(a)-(c), H&E stained sections of citrate-treated constructs immediately after printing show homogeneously distributed cells in a continuous porous silk fibroin matrix. Even distorted by the embedding and sectioning process, an open lumen is still clearly visible. The tube walls are porous, having two types of pores: one is the result of alginate removal by citrate treatment (irregular pores with poorly-defined edges), and the other is due to bubbles formed as a result of HRP catalyzed H_2O_2 decomposition (round, smooth-walled pores).

H&E stained sections of cultured constructs at Day 50 (Figure 6(d)-(f)) show dense cellular regions around the tube inner and outside surfaces, with comparatively few cells in the wall interior. While the construct still retains its original tubular shape during incubation (Figures 2(c) and 6(d) inset), it may be distorted during sectioning as seen from Figure 6(d). Nevertheless, the silk fibroin matrix is intact and porous after 50 days in culture. Deep blue nuclei are visible throughout the constructs, but there is an obvious difference between the surfaces of the tube, where multiple layers of densely packed cells are present in and over the pores, and the wall interior, where most of the pores are empty. As discussed earlier, the difference in cell density is likely due to faster proliferation at the surface, where the population is in contact with the surrounding media, than in the wall interior, where nutrient and oxygen diffusion is limited. Therefore, cell proliferation in the wall interior is limited by nutrition and oxygen and slower than on the surfaces of constructs. This disparity becomes significant over time as the surface cell density increases and nutrients and oxygen are consumed before they reach the wall interior. Similar dense surface/sparse interior cell populations in engineered constructs have been observed elsewhere and may be mitigated in future studies by dynamic, rather than static, culture of printed constructs[53].

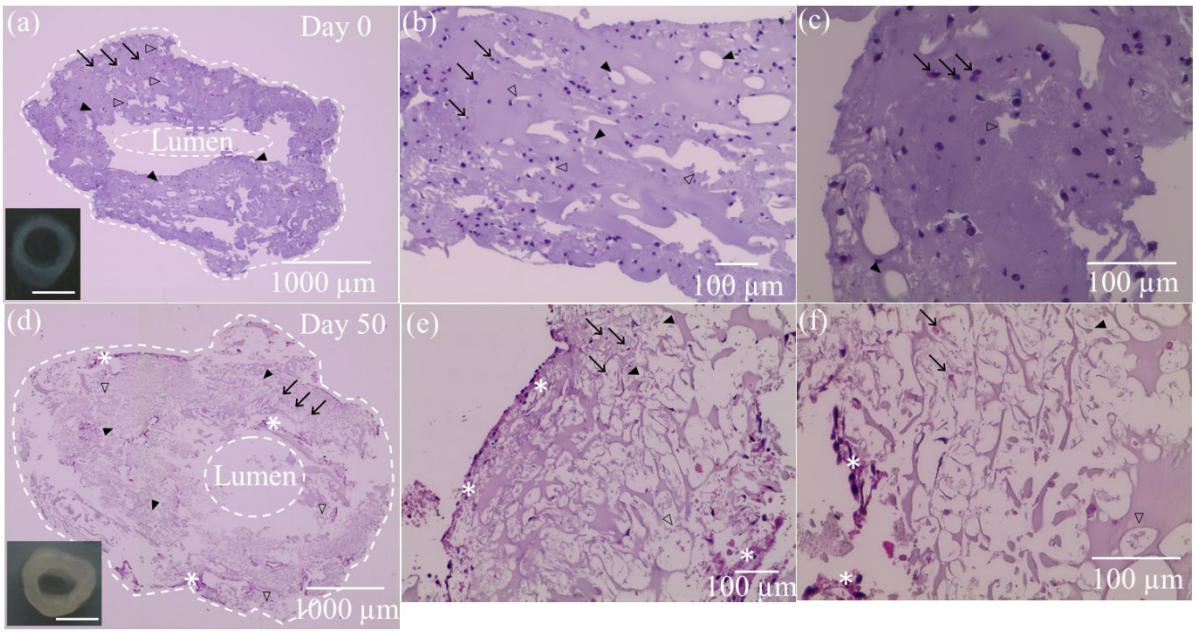

Figure 6. H&E stained sections of two citrate-treated constructs: (a-c) immediately after printing, and (d-f) after 50 days. Legend: ▲indicates pores from alginate loss, Δ indicates pores from bubbles, → indicates isolated cells in wall interior, and * indicates the peripheral dense cell region. (The constructs may be slightly distorted during sectioning; their physical shapes before sectioning can be seen in the insets; scale bars: 3 mm)

4. Conclusions

This study demonstrates that well-defined cell-laden silk fibroin hydrogel constructs can be fabricated by droplet-based 3D inkjet printing using alginate as a sacrificial material. Incorporation of alginate during the printing process is essential for well-defined constructs since the HRP catalyzed crosslinking of tyrosine residues in silk fibroin is too slow, and alginate in printed constructs can be removed using sodium citrate. It is concluded that the proposed two-step gelation-based inkjetting technique is an effective and efficient approach for 3D silk fibroin printing. Printed silk fibroin constructs are suitable for long term culture since cells continue

proliferating and remain metabolically active within structurally stable constructs. Removal of alginate from the printed constructs by immediate citrate treatment has little impact on cell morphology or long-term metabolic activity compared with constructs from which alginate is not actively removed. As such, the removal of alginate may be not necessary, especially, when biodegradable alginate is used.

The combination of silk fibroin's outstanding physical and mechanical properties with this freeform fabrication process will enable on-demand production of silk fibroin-based living tissue analogues suitable for a wide range of *in vitro* and *in vivo* applications. Future plans include improving the compatibility of silk and alginate to prevent demixing, printing heterogeneous constructs, encapsulating more clinically relevant cell types, development of dynamic culture facilities to promote vascular function, and more extensive biological characterization of printed constructs including temporally and spatially resolved live/dead imaging, H&E staining at intermediate time points, extracellular matrix production, and cell type-specific functionalities. While alginate is selected as the sacrificial material in this study due to its rapid gelation, other sacrificial materials may also be explored.

Acknowledgements

This work was partially supported by the US National Science Foundation (NSF CMMI-1634755). Histology samples were prepared by the Molecular Pathology Core at the College of Medicine, University of Florida. The authors acknowledge W. Chai for cell culture assistance and B. Davis for SEM support.

References

(1) Horch, R. E. Future Perspectives in Tissue Engineering: 'Tissue Engineering' Review Series. *J. Cell. Mol. Med.* **2006**, 10(1), 4-6, DOI: 10.1111/j.1582-4934.2006.tb00286.x.

(2) Ringeisen, B.R.; Pirlo, R.K.; Wu, P.K.; Boland, T.; Huang, Y.; Sun, W.; Hamid, Q.; Chrisey, D. B. Cell and Organ Printing Turns 15: Diverse Research to Commercial Transitions. *MRS Bull.* **2013,** 38(10), 834-843, DOI: 10.1557/mrs.2013.209.

(3) Huang, Y.; Leu. M.C.; Mazumder, J.; Donmez, A. Additive Manufacturing: Current State, Future Potential, Gaps and Needs, and Recommendations. *ASME J. of Manufacturing Sci. and Eng.* **2015**, 137(1), 014001-1-10, DOI: 10.1115/1.4028725.

(4) Murphy, S. V.; Atala, A. 3D Bioprinting of Tissues and Organs. *Nat. Biotechnol.* **2014**, 32(8), 773-785, DOI: 10.1038/nbt.2958.

(5) Pati, F.; Gantelius, J.; Svahn, H. A. 3D Bioprinting of Tissue/Organ Models. *Angew. Chem., Int. Ed.* **2016**, 55(15), 4650-4665, DOI: 10.1002/anie.201505062.

(6) Riggs, B.C.; Dias, A.D.; Schiele, N.R.; Cristescu, R.; Huang, Y.; Corr, D.T.; Chrisey, D.B. Matrix-Assisted Pulsed Laser Methods for Biofabrication. *MRS Bull.* **2011**, 36(12), 1043-1050, DOI: 10.1557/mrs.2011.276.

(7) Chan, V.; Jeong, J.H.; Bajaj, P.; Collens, M.; Saif, T.; Kong, H.; Bashir, R. Multi-material Bio-Fabrication of Hydrogel Cantilevers and Actuators with Stereolithography. *Lab Chip* **2012**, 12(1), 88-98, DOI: 10.1039/C1LC20688E.

(8) Xu, C.; Chai, W.; Huang, Y.; Markwald, R.R. Scaffold-Free Inkjet Printing of Three-Dimensional Zigzag Cellular Tubes. *Biotechnol. Bioeng.* **2012**, 109(12), 3152-3160, DOI: 10.1002/bit.24591.

(9) Christensen, K.; Xu, C.; Chai, W.; Zhang, Z.; Fu, J.; Huang, Y. Freeform Inkjet Printing of Cellular Structures with Bifurcations. *Biotechnol. Bioeng.* **2015**, 112(5), 1047-1055, DOI: 10.1002/bit.25501.

(10) Xiong, R.; Zhang, Z.; Chai, W.; Huang, Y.; Chrisey, D.B. Freeform Drop-on-Demand Laser Printing of 3D Alginate and Cellular Constructs. *Biofabrication* **2015**, 7(4), 045011-1-13, DOI: 10.1088/1758-5090/7/4/045011.

(11) Jin, Y.; Compaan, A.; Bhattacharjee, T.; Huang, Y. Granular Gel Support-Enabled Extrusion of Three-Dimensional Alginate and Cellular Structures. *Biofabrication* **2016**, 8(2), 025016, DOI: 10.1088/1758-5090/8/2/025016.

(12) Ma, X.; Qu, X.; Zhu, W.; Li, Y.S.; Yuan, S.; Zhang, H.; Liu, J.; Wang, P.; Lai, C.S.E.; Zanella, F.; Feng, G.S. Deterministically Patterned Biomimetic Human iPSC-Derived Hepatic Model via Rapid 3D Bioprinting. *Proc. Natl. Acad. Sci. U. S. A.* **2016**, 113(8), 2206-2211, DOI: 10.1073/pnas.1524510113.

(13) Malda, J.; Visser, J.; Melchels, F.P.; Jüngst, T.; Hennink, W.E.; Dhert, W.J.; Groll, J.; Hutmacher, D. W. 25th Anniversary Article: Engineering Hydrogels for Biofabrication. *Adv. Mater. (Weinheim, Ger.)* **2013**, 25(36), 5011-5028, DOI: 10.1002/adma.201302042.

(14) Jungst, T.; Smolan, W.; Schacht, K.; Scheibel, T.; Groll, J. Strategies and Molecular Design Criteria for 3D Printable Hydrogels. *Chem. Rev.* **2015**, 116(3), 1496-1539, DOI: 10.1021/acs.chemrev.5b00303.

(15) Stanton, M. M.; Samitier, J.; and Sánchez, S. Bioprinting of 3D hydrogels. *Lab Chip* **2015**, 15(15), 3111-3115, DOI: 10.1039/C5LC90069G.

(16) Jose, R. R.; Rodriquez, M. J.; Dixon, T. A.; Omenetto, F. G.; Kaplan, D. L. Evolution of Bioinks and Additive Manufacturing Technologies for 3D Bioprinting. *ACS Biomater. Sci. Eng.* **2016**, in press, DOI: 10.1021/acsbiomaterials.6b00088.

(17) Grassl, E. D.; Oegema, T. R.; Tranquillo, R. T. A Fibrin-Based Arterial Media Equivalent. *J. Biomed. Mater. Res., Part A* **2002,** 66(3), 550-561, DOI: 10.1002/jbm.a.10589.

(18) Murphy, A. R.; Kaplan, D. L. Biomedical Applications of Chemically-Modified Silk Fibroin. *J. Mater. Chem.* **2009**, 19(36), 6443-6450, DOI: 10.1039/B905802H.

(19) Kundu, B.; Kurland, N. E.; Bano, S.; Patra, C.; Engel, F. B.; Yadavalli, V. K.; Kundu, S. C. Silk Proteins for Biomedical Applications: Bioengineering Perspectives. *Prog. Polym. Sci.* **2014**, 39(2), 251-267, DOI: 10.1016/j.progpolymsci.2013.09.002.

(20) Rockwood, D. N.; Preda, R. C.; Yücel, T.; Wang, X.; Lovett, M. L.; Kaplan, D. L. Materials Fabrication from Bombyx mori Silk Fibroin. *Nat. Protoc.* **2011**, 6(10), 1612-1631, DOI: 10.1038/nprot.2011.379.

(21) Abbott, R. D.; Kimmerling, E. P.; Cairns, D. M.; Kaplan, D. L. Silk as a Biomaterial to Support Long-Term Three-Dimensional Tissue Cultures. *ACS Appl. Mater. Interfaces* **2016**, Article ASAP, DOI: 10.1021/acsami.5b12114.

(22) Horan, R.L.; Antle, K.; Collette, A.L.; Wang, Y.; Huang, J.; Moreau, J.E.; Volloch, V.; Kaplan, D.L.; Altman, G. H. In vitro Degradation of Silk Fibroin. *Biomaterials* **2005**, 26(17), 3385-3393, DOI: 10.1016/j.biomaterials.2004.09.020.

(23) Wang, Y.; Rudym, D.D.; Walsh, A.; Abrahamsen, L.; Kim, H.J.; Kim, H.S.; Kirker-Head, C.; Kaplan, D. L. In vivo Degradation of Three-Dimensional Silk Fibroin Scaffolds. *Biomaterials* **2008**, 29(24), 3415-3428, DOI: 10.1016/j.biomaterials.2008.05.002.

(24) Bellas, E.; Lo, T. J.; Fournier, E.P.; Brown, J. E.; Abbott, R. D.; Gil, E.S.; Marra, K. G.; Rubin, J. P.; Leisk, G. G.; Kaplan, D.L. Injectable Silk Foams for Soft Tissue Regeneration. *Adv. Healthcare Mater.* 2015, 4 (3), 452-459, DOI: 10.1002/adhm.201400506.

(25) Singh, R.; Sarker, B.; Silva, R.; Detsch, R.; Dietel, B.; Alexiou, C.; Boccaccini, A.R.; Cicha, I. Evaluation of Hydrogel Matrices for Vessel Bioplotting: Vascular Cell Growth and Viability. *J. Biomed. Mater. Res., Part A* **2015**, 104(3), 577-585, DOI: 10.1002/jbm.a.35590.

(26) Partlow, B.P.; Hanna, C.W.; Rnjak-Kovacina, J.; Moreau, J.E.; Applegate, M.B.; Burke, K.A.; Marelli, B.; Mitropoulos, A.N.; Omenetto, F.G.; Kaplan, D. L. Highly Tunable Elastomeric Silk Biomaterials. *Adv. Funct. Mater.* **2014**, 24(29), 4615-4624, DOI: 10.1002/adfm.201400526.

(27) Yucel, T.; Cebe, P.; Kaplan, D. L. Vortex-Induced Injectable Silk Fibroin Hydrogels. *Biophys. J.* 2009, 97(7), 2044-2050, DOI: 10.1016/j.bpj.2009.07.028.

(28) Das, S.; Pati, F.; Choi, Y.J.; Rijal, G.; Shim, J.H.; Kim, S.W.; Ray, A.R.; Cho, D.W.; Ghosh, S. Bioprintable, Cell-Laden Silk Fibroin–Gelatin Hydrogel Supporting Multilineage Differentiation of Stem Cells for Fabrication of Three-Dimensional Tissue Constructs. *Acta Biomater.* **2015**, 11, 233-246, DOI: 10.1016/j.actbio.2014.09.023.

(29) Ghosh, S.; Parker, S. T.; Wang, X.; Kaplan, D. L.; Lewis, J. A. Direct-Write Assembly of Microperiodic Silk Fibroin Scaffolds for Tissue Engineering Applications. *Adv. Funct. Mater.* **2008**, 18(13), 1883-1889, DOI: 10.1002/adfm.200800040.

(30) Parker, S. T.; Domachuk, P.; Amsden, J.; Bressner, J.; Lewis, J. A.; Kaplan, D. L.; Omenetto, F. G. Biocompatible Silk Printed Optical Waveguides. *Adv. Mater. (Weinheim, Ger.)* **2009**, 21(23), 2411-2415, DOI: 10.1002/adma.200801580.

(31) Das, S.; Pati, F.; Chameettachal, S.; Pahwa, S.; Ray, A. R.; Dhara, S.; Ghosh, S. Enhanced Redifferentiation of Chondrocytes on Microperiodic Silk/Gelatin Scaffolds: Toward Tailor-Made Tissue Engineering. *Biomacromolecules* **2013,** 14(2), 311-321, DOI: 10.1021/bm301193t.

(32) Jose, R.; Brown, J.; Polido, K.; Omenetto, F. G.; Kaplan, D. L. Polyol-Silk Bio-ink Formulations as Two-part Room-Temperature Curable Materials for 3-D Printing. *ACS Biomater. Sci. Eng.* **2015**, 1(9), 780-788, DOI: 10.1021/acsbiomaterials.5b00160.

(33) Limem, S.; Calvert, P.; Kim, H. J.; Kaplan, D. L. Differentiation of Bone Marrow Stem Cells on Inkjet Printed Silk Lines. *Mater. Res. Soc. Symp. Proc.*, **2006,** 950, 0950-D04, DOI: 10.1557/PROC-0950-D04-18.

(34) Tao, H.; Marelli, B.; Yang, M.; An, B.; Onses, M.S.; Rogers, J.A.; Kaplan, D.L.; Omenetto, F. G. Inkjet Printing of Regenerated Silk Fibroin: From Printable Forms to Printable Functions. *Adv. Mater. (Weinheim, Ger.)* **2015**, 27(29), 4273-4279, DOI: 10.1002/adma.201501425.

(35) Xu, C.; Christensen, K.; Zhang, Z.; Huang, Y.; Fu, J.; Markwald, R.R. Predictive Compensation-Enabled Horizontal Inkjet Printing of Alginate Tubular Constructs. *Manuf. Lett.* **2013**, 1(1), 28-32, DOI: 10.1016/j.mfglet.2013.09.003.

(36) Xu, C.; Zhang, Z.; Christensen, K.; Huang, Y.; Fu, J.; Markwald, R. Freeform Vertical and Horizontal Fabrication of Alginate-Based Vascular-Like Tubular Constructs Using Inkjetting. *ASME J. of Manufacturing Sci. and Eng.* **2014**, 136(6), 061020-1-8, DOI: 10.1115/1.4028578.

(37) Tabriz, A. G.; Hermida, M. A.; Leslie, N. R.; Shu, W. Three-Dimensional Bioprinting of Complex Cell Laden Alginate Hydrogel Structures. *Biofabrication* **2015**, 7(4), 045012, DOI: 10.1088/1758-5090/7/4/045012.

(38) Zimmermann, H.; Shirley, S. G.; Zimmermann, U. Alginate-Based Encapsulation of Cells: Past, Present, and Future. *Curr. Diabetes Rep.* **2007**, 7(4), 314-320, DOI: 10.1007/s11892-007-0051-1.

(39) Solorio, L.; Zwolinski, C.; Lund, A. W.; Farrell, M. J.; Stegemann, J. P. Gelatin Microspheres Crosslinked with Genipin for Local Delivery of Growth Factors. *J. Tissue Eng. Regener. Med.* **2010**, 4(7), 514-523, DOI: 10.1002/term.267.

(40) de Moraes, M. A.; Silva, M. F.; Weska, R. F.; Beppu, M. M. Silk Fibroin and Sodium Alginate Blend: Miscibility and Physical Characteristics. *Mater. Sci. Eng., C* **2014,** 40, 85-91, DOI: 10.1016/j.msec.2014.03.047.

(41) Hu, M.; Kurisawa, M.; Deng, R.; Teo, C.M.; Schumacher, A.; Thong, Y.X.; Wang, L.; Schumacher, K.M.; Ying, J. Y. Cell Immobilization in Gelatin–Hydroxyphenylpropionic Acid Hydrogel Fibers. *Biomaterials* **2009**, 30(21), 3523-3531, DOI: 10.1016/j.biomaterials.2009.03.004.

(42) Zhu, M.; Wang, K.; Mei, J.; Li, C.; Zhang, J.; Zheng, W.; An, D.; Xiao, N.; Zhao, Q.; Kong, D.; Wang, L. Fabrication of Highly Interconnected Porous Silk Fibroin Scaffolds for Potential Use as Vascular Grafts. *Acta Biomater.* 2014, 10(5), 2014-2023, DOI: 10.1016/j.actbio.2014.01.022.

(43) Zhang, H.; Liu, X.; Yang, M.; Zhu, L. Silk Fibroin/Sodium Alginate Composite Nano-Fibrous Scaffold Prepared Through Thermally Induced Phase-Separation (TIPS) Method for Biomedical Applications. *Mater. Sci. Eng., C* 2015, 55, 8-13, DOI: 10.1016/j.msec.2015.05.052.

(44) Unger, R. E.; Wolf, M.; Peters, K.; Motta, A.; Migliaresi, C.; Kirkpatrick, C. J. Growth of Human Cells on a Non-Woven Silk Fibroin Net: a Potential for Use in Tissue Engineering. *Biomaterials* **2004**, 25(6), 1069-1075, DOI: 10.1016/S0142-9612(03)00619-7.

(45) Wang, X.; Kluge, J. A.; Leisk, G. G.; Kaplan, D. L. Sonication-Induced Gelation of Silk Fibroin for Cell Encapsulation. *Biomaterials* 2**008**, 29(8), 1054-1064, DOI: 10.1016/j.biomaterials.2007.11.003.

(46) Minoura, N.; Aiba, S. I.; Higuchi, M.; Gotoh, Y.; Tsukada, M.; Imai, Y. Attachment and Growth of Fibroblast Cells on Silk Fibroin. *Biochem. Biophys. Res. Commun.* **1995**, 208(2), 511-516, DOI: 10.1006/bbrc.1995.1368.

(47) Servoli, E.; Maniglio, D.; Motta, A.; Predazzer, R.; Migliaresi, C. Surface Properties of Silk Fibroin Films and Their Interaction with Fibroblasts. *Macromol. Biosci.* **2005**, 5(12), 1175-1183, DOI: 10.1002/mabi.200500137.

(48) Lee, J.; Cuddihy, M. J.; Kotov, N. A. Three-Dimensional Cell Culture Matrices: State of the Art. *Tissue Eng., Part B* **2008**, 14(1), 61-86, DOI: 10.1089/teb.2007.0150.

(49) Wan, A. C. Recapitulating Cell–Cell Interactions for Organoid Construction–Are Biomaterials Dispensable? *Trends Biotechnol.* **2016**, in press, DOI: 10.1016/j.tibtech.2016.02.015.

(50) Alsberg, E.; Anderson, K. W.; Albeiruti, A.; Franceschi, R. T.; Mooney, D. J. Cell-Interactive Alginate Hydrogels for Bone Tissue Engineering. *J. Dent. Res.* **2016**, 80(11), 2025-2029, DOI: 10.1177/00220345010800111501.

(51) Burdick, J. A.; Anseth, K. S. Photoencapsulation of Osteoblasts in Injectable RGD-Modified PEG Hydrogels for Bone Tissue Engineering. *Biomaterials* 2002, 23(22), 4315-4323, DOI: 10.1016/S0142-9612(02)00176-X.

(52) Zahir, N.; Weaver, V. M. Death in the Third Dimension: Apoptosis Regulation and Tissue Architecture. *Curr. Opin. Genet. Dev.* **2004**, 14(1), 71-80, DOI: 10.1016/j.gde.2003.12.005.

(53) Ghezzi, C. E.; Marelli, B.; Donelli, I.; Alessandrino, A.; Freddi, G.; Nazhat, S. N. The Role of Physiological Mechanical Cues on Mesenchymal Stem Cell Differentiation in an Airway Tract-Like Dense Collagen–Silk Fibroin Construct. *Biomaterials*, **2014**, 35(24), 6236-6247, DOI: 10.1016/j.biomaterials.2014.04.040.